IGHEM - Montreal 1996

CFD-Calculations of the protrusion effect and impact on the acoustic discharge measurement accuracy

Alex Voser
Swiss Federal Institute of Technology in Zürich
ETH-Z, Turbomachinery Laboratory, CH-8092 Zürich, Switzerland
Tel. +411 632 67 85, Fax +411 632 11 00
Email: voser@iet.mavt.ethz.ch

Summary

The velocity distribution around ACCUSONIC 7600 feed through transducers has been computed in a turbulent boundary layer using the commercial available CFD system „TASCflow". Because the variations in the computed flow field were small in the investigated range of Reynolds numbers, the influence of the protrusion on the mean path velocity could be expressed with only two parameters: the affected path length ℓ and a protrusion coefficient f. With these two parameters, measurements with an eight path flowmeter have been numerically simulated in hydraulic smooth and rough conduits and in the transition region. The measurement error was calculated in function of the conduit diameter, the wall roughness and the Reynolds number for fully developed turbulent velocity profiles. The results show that for large conduits in conjunction with low Reynolds numbers as well as for very small conduits the expected measurement error due to the protrusion may become larger than ±0.5%.

Résumé

La répartition de vitesses autour de capteurs acoustiques du type 7600 de ACCUSONIC a été calculée en utilisant „TASCflow", un logiciel CFD. Comme les différences entre les champs de vitesses calculées étaient faibles dans la gamme de nombres Reynolds étudiée, l' influence de la protrusion sur la vitesse moyenne le long de la piste acoustique a pu être exprimé que par deux paramètres, la longueur de la piste influencée ℓ et le coefficient de protrusion f. Avec ces deux paramètres, des mesures avec un débitmètre acoustique a huit pistes ont été simulés numériquement dans des conduites lisses, rugueuses et dans la zone de transition avec le but de calculer les erreurs de mesures en fonction du diamètre de la conduite, de la rugueusité et du nombre Reynolds pour des écoulements turbulents développés. Les résultats montrent les erreurs due a la protrusion dépassent les ±0.5% pour des conduites avec de gros diamètres combinées avec de petits nombres Reynolds ou pour des conduites très petites.

1. Introduction

In practical applications of the **A**coustic **D**ischarge **M**easurement (ADM) the acoustic transducers are very often slightly protruding into the conduit. Because the underlying theory of the calculation of the mean path velocities and the integration of the individual path velocities is based on protrusion-free transducers, measurement errors due to the transducer protrusion have to be taken into account.
A first effect of the protrusion arises from the neglect of the smaller boundary layer velocities compared to the velocities in the core region of the conduit. This yields in a higher acoustic path mean velocity in contrast to a theoretical path starting and ending at the conduit wall and therefore an over-estimation of the actual discharge depending on the ratio of protrusion e/D. This effect is easy to simulate numerically and has already been investigated by Grego[1], Sugishita et al.[2] and Voser et al.[3].

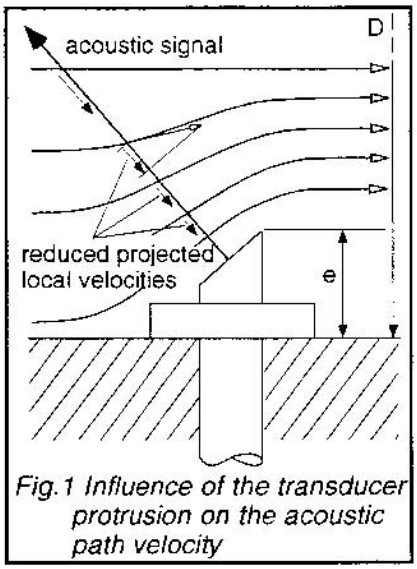

Fig.1 Influence of the transducer protrusion on the acoustic path velocity

The second effect consists of the local distortion of the velocity profile around the transducers shown in Fig.1. In both cases - for upstream and downstream transducers - the mean path velocity is reduced due to the smaller velocities projected along the acoustic path.
The comparison of different discharge measurement methods (for an overview see Staubli/Graf[4]) show a certain statistic evidence that this effect must compensate the first effect described above in the ADM. For a verification of this assumption we have studied the velocity distribution in the vicinity of to the acoustic transducers using numerical calculations and laboratory experiments. Because of their widespread use, the investigation was performed on the 7600 type feed through transducers from ACCUSONIC.

2. Numerical computation of the local flow field with a CFD-Code

To simulate real installation conditions, we have calculated the local flow fields of inner and outer path transducers mounted on the upstream and downstream side of the flowmeter section. The transducers were „mounted" in conduits with a diameter of 1 and 2 meters and a axial mean velocities of 1, 2, and 5 m/s. For practical reasons only relevant details of the transducers have been modelled accurately, others have been simplified or neglected.

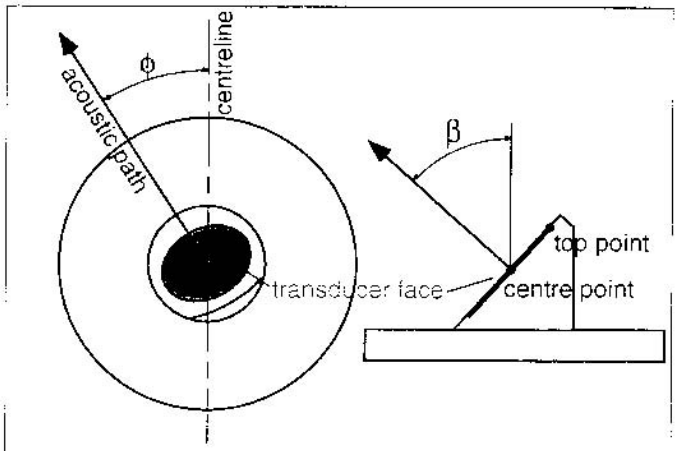

Fig.2 Transducer face and rotation angle φ

Like in a real installation the transducers had to be rotated with respect to the centreline. The rotation angle ϕ can be approximately calculated from the path angle φ and the head angle β with

$$\theta \approx \arccos\left(\frac{\cos\varphi}{\sin\beta}\right). \qquad (1)$$

The computations have been carried out with TASCflow™ from ASC, a software system for solving fluid flow problems in industrial and research areas. TASCflow is based on a 3D finite volume solver relying on the compressible time-averaged Navier-Stokes equations and the k-ε closure equations.

3. Grid generation

The grid with a total of 70'000 grid points presented in Fig.3 was generated using TASCgrid, a module of TASCflow. With TASCflow supporting multi-block grids we divided the grid in three blocks:

- *Conduit* To save grid points, only a radial 90° section consisting of about 10'000 grid points has been modelled. Symmetry boundary conditions were applied to the long sides of the section. To ensure a fully developed turbulent flow profile at the regions of interest, the length of the conduit was set to 40 diameters and the transducer placed near the end of the conduit.
- *Transducer* Four individual grids with about 50'000 grid points each take into account the different positions and geometries of the transducers. The grid had to be refined at places with high gradients to improve the convergence of the flow prediction.
- *Transducer vicinity* Because of the higher gradients especially in the wake of the transducers the conduit grid in the vicinity of the transducer had to be refined locally yielding in additional 10'000 grid points.

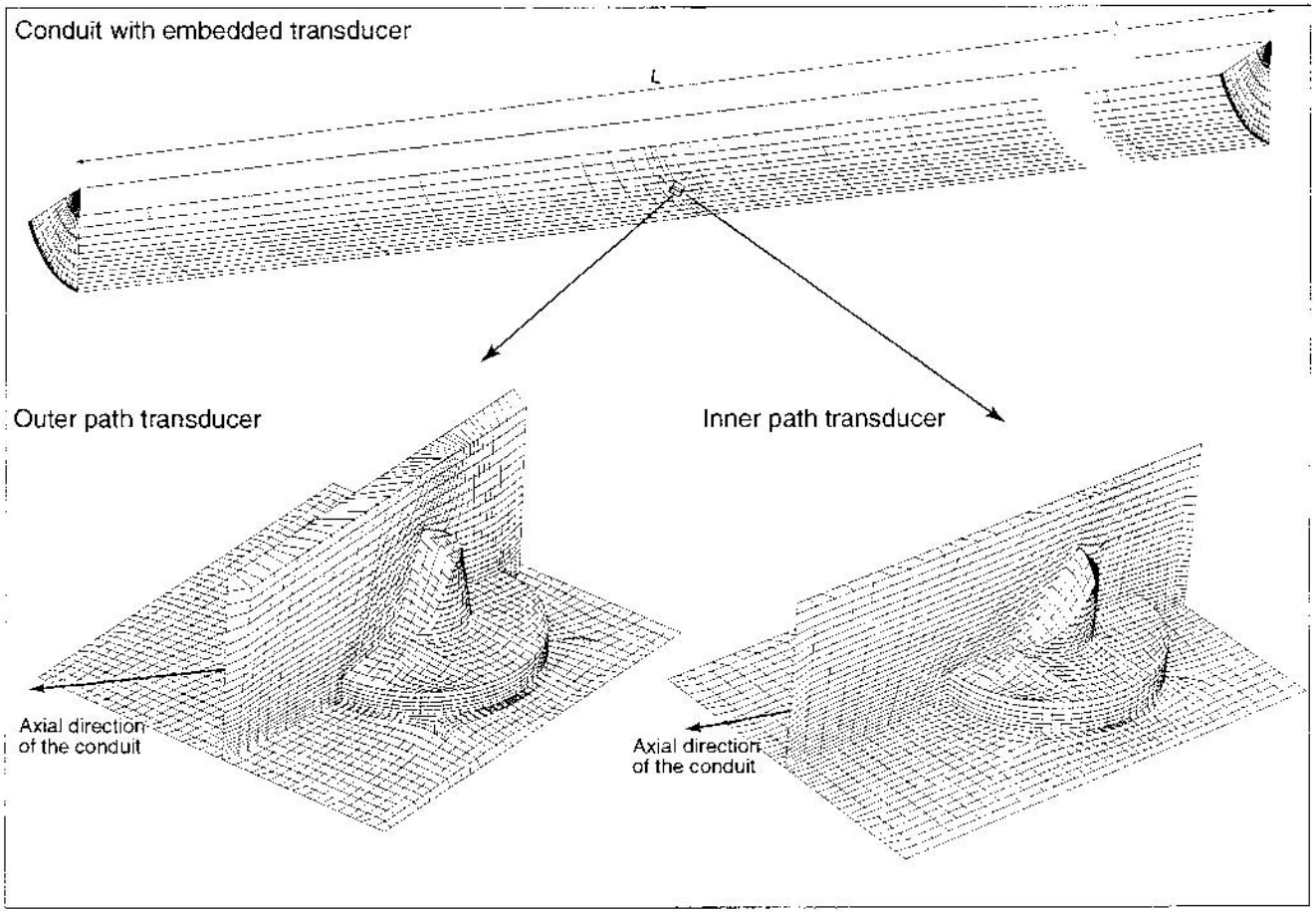

Fig.3 Conduit and transducer grids

4. Calculation of the local flow field and the projected path velocity

As an example of a typical flow field in the transducer vicinity Fig.4 shows the calculated axial velocity distribution for an outer path upstream transducer. A large recirculation zone exists behind the transducer face which affects the acoustic signal and therefore the measurement uncertainties of the ADM. Fortunately the height of this zone is not much higher than the transducer itself.

	path length affected [m]	protrusion coefficient	
		CFD	*LDA*
Outer paths			
downstream	$\ell_{oD} = 0.156$	$f_{oD} = 0.90$	
upstream	$\ell_{oU} = 0.088$	$f_{oU} = 0.83$	
Inner paths			
downstream	$\ell_{iD} = 0.210$	$f_{iD} = 0.93$	$f_{iD} = 0.94$
upstream	$\ell_{iU} = 0.115$	$f_{iU} = 0.86$	$f_{iU} = 0.85$

Table 1 Parameters characterising the flow field distortion along the acoustic path

Although the boundary profile in the vicinity of the transducer was slightly different than the boundary profile simulated with CFD the agreement between the experimental and numerical results is excellent. Therefore we assumed that these coefficients have an general character (for an 7600 type transducer) and can be applied to the full range of Reynolds numbers and wall roughnesses found in hydraulic powerplants.

5. Simulation of the ADM with the protrusion effect

Measurements with an eight path flowmeter were simulated assuming a fully developed turbulent velocity distribution $v_{Turb}(s)$ in hydraulic rough and smooth conduits and in the transition region between (Schlichting[5]). For the smooth conduit, we used a velocity profile consisting of three layers; for the other two cases simple logarithmic functions were applied.

To calculate the mean path velocity, we divided the path into three parts (see Fig.6). Using the definition (2) of the protrusion coefficient f the local mean velocities at the ends of the path have been weighted with f and then summed up together with the local mean velocity of the core region. This is illustrated in the following equation valid for the inner paths and a path angle of 45°:

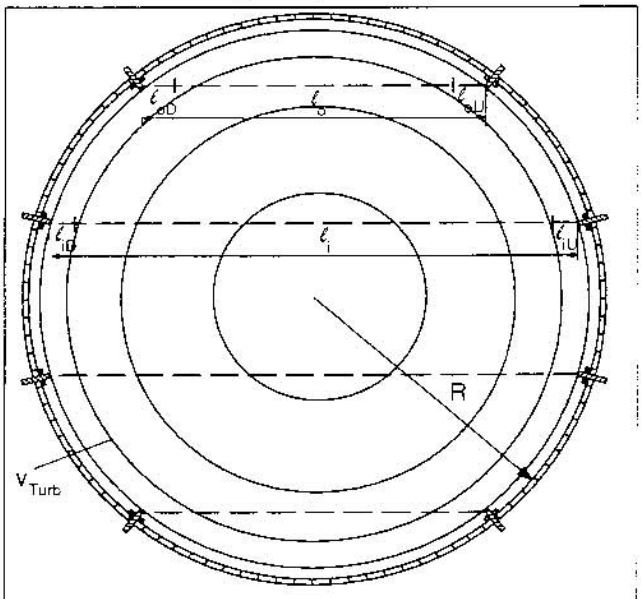

Fig.6 Simulation of the ADM in a fully developed flow field with protruding transducers

$$\overline{v}_i = \frac{f_{iD}\int_0^{\ell'_{iU}} v_{Turb}(s)\,ds + \int_{\ell'_{iU}}^{\ell_i-\ell'_{iD}} v_{Turb}(s)\,ds + f_{iU}\int_{\ell_i-\ell'_{iD}}^{\ell_i} v_{Turb}(s)\,ds}{\ell_i};\quad \ell'_{iU} = \ell_{iU}\cos 45°,\ \ell'_{iD} = \ell_{iD}\cos 45° \qquad (3)$$

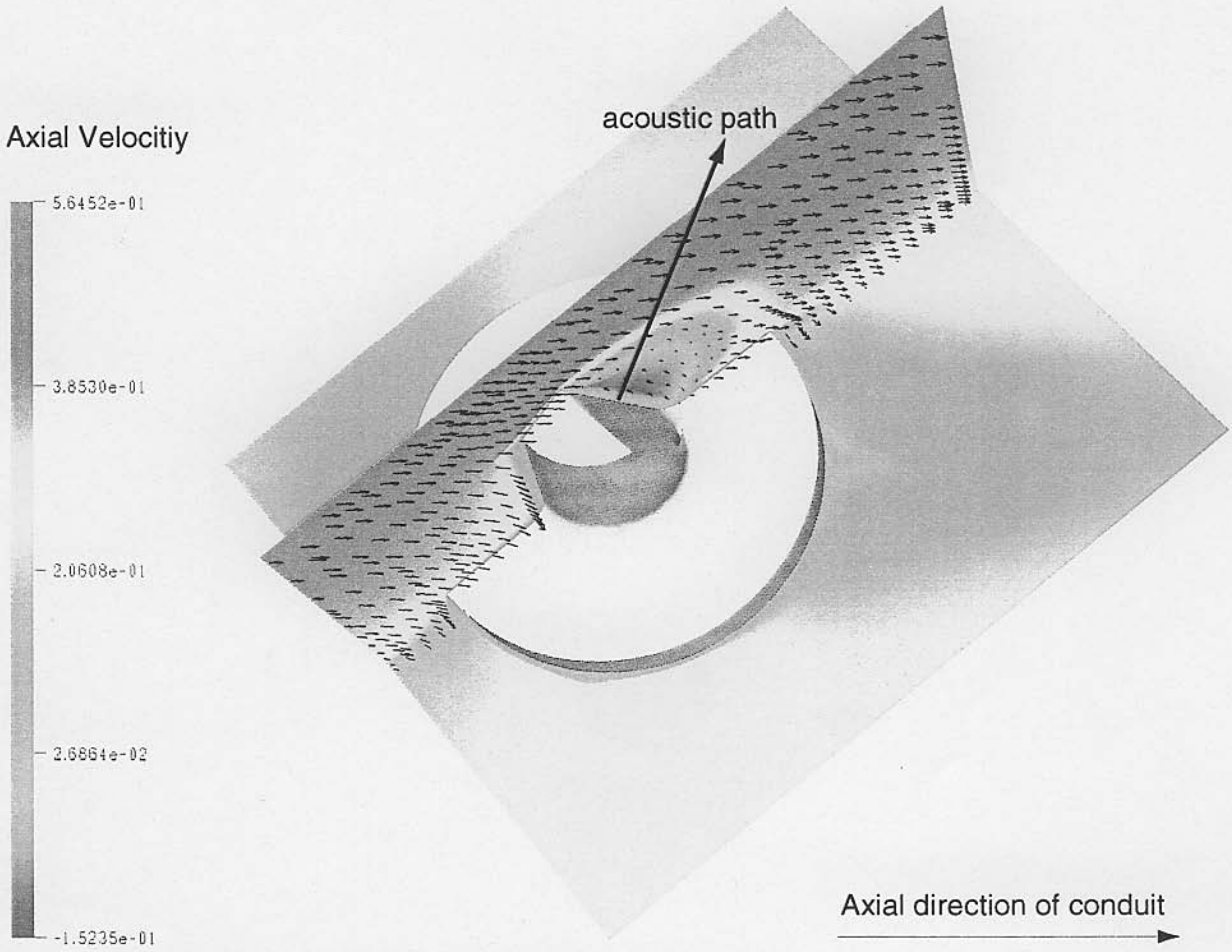

Fig.4 Axial velocity distribution for an outer downstream transducer

Of greatest interest is the local velocity projected onto the acoustic path affecting directly the travel time of the acoustic signal along the acoustic path. Fig.5 shows the projected velocities for all cases calculated compared to the non-disturbed velocity profile also projected onto the acoustic path. For the calculations we assumed that the acoustic path starts at the centre of the transducer face, a point which is currently undefined: a signal starting from the top of the transducer face (see Fig.2) will be less influenced by the local flow field distortion and therefore - depending on the acoustic path direction - reach the opposite transducer earlier or delayed. Depending on the inertia of the receiving transducer membrane, the transducer alignment, the detection method and the detection threshold this weaker signal from the top could be detected first even if it is weaker than a signal coming from the centre.

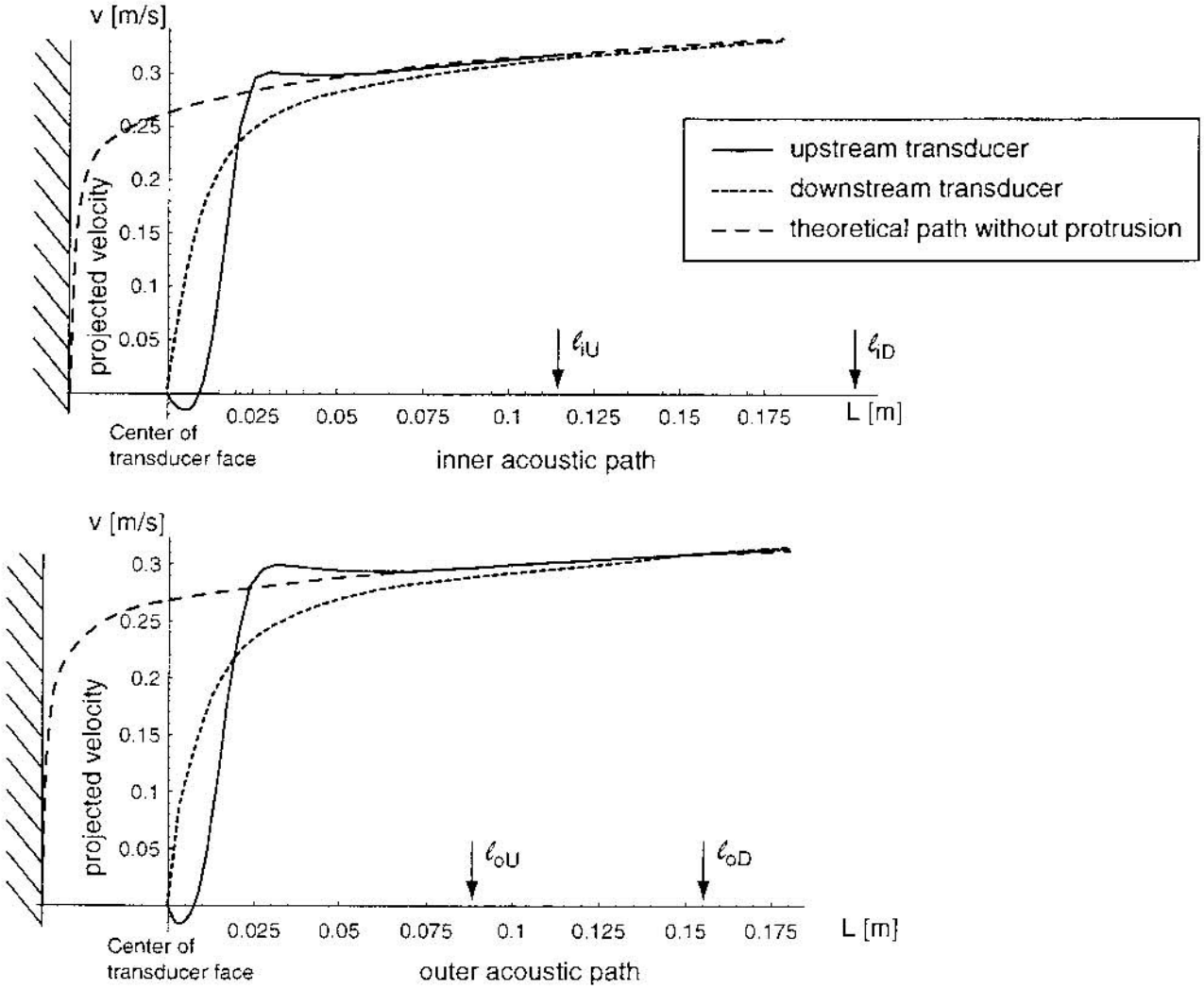

Fig.5 Projected acoustic path velocities for a Reynolds number of 10^6

The results have shown that the ratio of the projected velocities with protrusion $v_{proj}(s)$ and without protrusion (v_{proj}) and of their integrals are barely influenced by the Reynolds number in the investigated range. Based on this result, we characterised the distribution of the projected velocities with a single pair of parameters for each of the four cases. One parameter is the path length ℓ up to the point, where the projected velocities with and without protrusion converge to less than 0.1%. The other parameter called protrusion coefficient f is calculated from the ratio of the integrated projected velocities with and without protrusion. For an outer, downstream transducer this becomes

$$f_{oD} = \frac{\int_0^{\ell_{oD}} v_{proj_e}(s)\,ds}{\int_0^{\ell_{oC}} v_{proj}(s)\,ds} \qquad (2)$$

Table 1 gives an overview on all parameters. For comparison purposes, values obtained by 2D Laser Doppler Anemometer (LDA) measurements in a open water channel are also presented.

To compare the results with already performed laboratory and field measurements, the individual path velocities were integrated using the Gauss-Jacobi integration method according to IEC41. With the actual discharge the measurement uncertainty in function of the Reynolds number Re, the wall roughness ks and the conduit diameter was computed. Fig.7 shows the measurement uncertainties for 0.9 m and Fig.8 for a 2.5 m conduit.

Unfortunately it is quite difficult to estimate the sand roughness of the conduit in real installations. Typical values for steel conduits are between 0.03 and 0.1 mm, whereas concrete conduits have values above 0.3 mm.

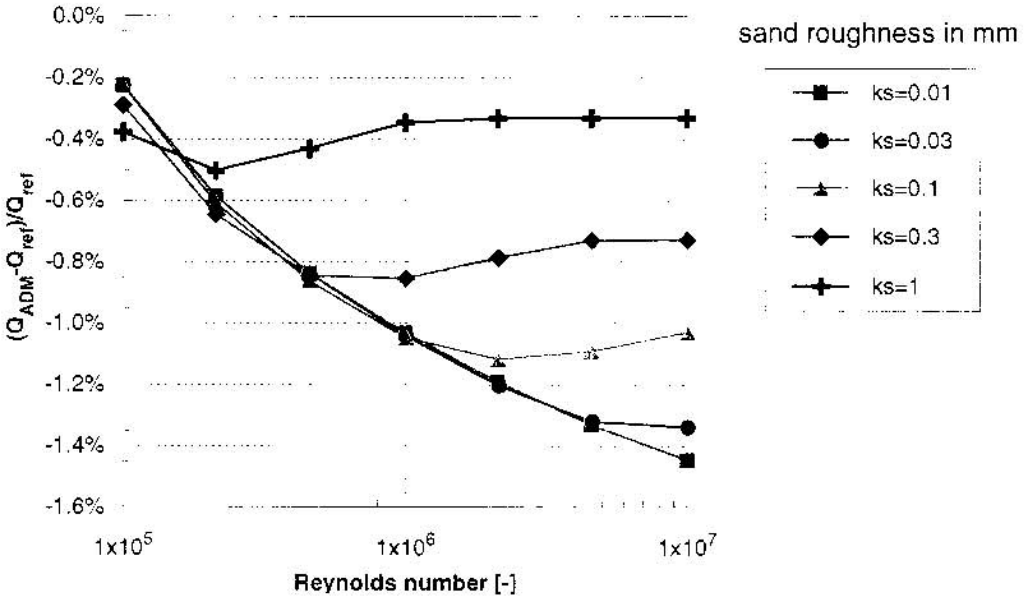

Fig.7 Measurement uncertainties due to protrusion in a 0.9 m conduit

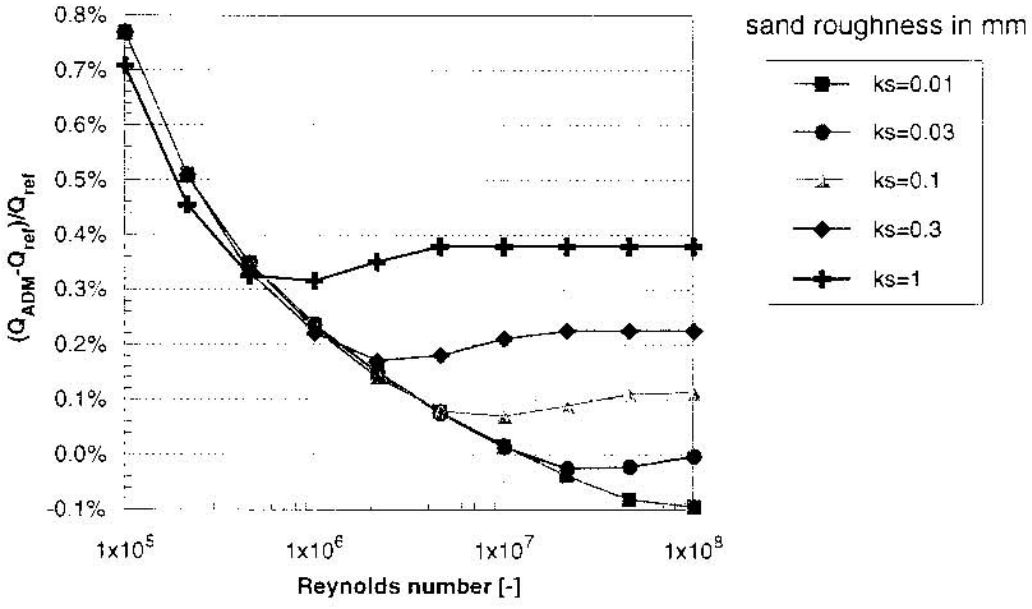

Fig.8 Measurement uncertainties due to protrusion in a 2.5 m conduit

6. Conclusions

- When using 7600 type transducers and a path angle of 45°, the protrusion error is smaller than ±0.5% for diameters larger than 2 m except for velocities below 0.1 m/s. The range of the measurement errors decreases with increasing diameter. Laboratory measurements with very small conduit diameters with the same transducers will show more significant errors, however exact knowledge of the wall roughness and fully developed velocity profile is then required to compare with the errors shown in Fig.8.
- With a path angle of 65°, the mean path velocity will be increased because the acoustic path leaves the disturbed zone faster than with 45° paths. Therefore the measurement errors will be shifted more to positive values.
- A built-in discharge correction in the flowmeter will be possible only in few cases, because very often the flow field in the measuring section is disturbed and therefore also the velocity distribution in the boundary layer will be unknown. Computed measurement errors from investigations with fully developed profiles like those presented in this paper should then be included as additional measurement uncertainties.
- In a future investigation it should be verified whether the assumption holds, that the acoustic path starts and ends at the centre of the transducer face.

References

[1] G. Grego
Pipeline flowrate measurements intercomparison tests of current meters and a multipath acoustic flowmeter
I.C.M.G. 18th Meeting, Dubrovnik, 8-11 Sept. 1987

[2] K. Sugishita, T. Mototki, T. Kosugi
Correction method to improve the accuracy of multipath acoustic flowmeters
16th Symposium of the IAHR , Sao Paulo, September 1993

[3] Voser A., Bruttin Ch., Prénat J.-E., Staubli T.,
Improving acoustic flow measurement
International Water Power & Dam Construction, April 1996

[4] T. Staubli, K. Graf
Akustische Durchflussmessung in Wasserkraftanlagen.
wasser, energie, luft 7/8 1992 (in German)

[5] H. Schlichting
Grenzschicht-Theorie
Verlag G. Braun, Karlsruhe 1982

Acknowledgement

LDA Measurements: P. Billeter, Versuchsanstalt für Wasserbau (VAW), ETH Zürich

Funding: NEFF (Swiss National Energy Foundation)